Active Balancing of a Supercritical Rotor on Active Magnetic Bearings *

Kai Adler, Christoph Schalk, Rainer Nordmann
Mechatronics in Mechanical Engineering
Darmstadt University of Technology
Petersenstraße 30, 64287 Darmstadt, Germany
adler@mum.tu-darmstadt.de
nordmann@mum.tu-darmstadt.de

Beat Aeschlimann
Mecos Traxler AG
Industriestraße 26, 8404 Winterthur, Switzerland
beat.aeschlimann@mecos.com

***Abstract*— Balancing of rotors needs a lot of manpower, specific knowledge and is time-consuming. In the rising field of high speed machinery also the requirements for suitable effective balancing concepts increase. Here a combination of active magnetic bearings (AMBs) and active balancing devices (ABDs) on a supercritical rotor creates the possibility for a partial automation of the balancing process. That way critical rotor speeds can be passed and the time effort for the balancing process can be reduced significantly.**

***Index Terms*— Active Balancing - Supercritical Rotor - Active Magnetic Bearings - Active Balancing Device**

I. Introduction

Active magnetic bearings (AMBs) give a lot of advantages due to their contactless operation. Especially the field of high speed machinery is predestinated for the use of AMBs because their benefit rises with the operating speed. An unwanted effect of the high speeds are the increasing excitations by unbalance forces caused by geometrical imperfections and inhomogeneity of material. Higher vibration levels yield to a live time reduction and an increase of service effort. Furthermore saturation of the AMBs will take any possibility to react to other excitations. At the final end the target operating speed can not be reached especially in case, when it is supercritical. To avoid all this negative effects it is essential to balance all rotating parts. Balancing needs a lot of manpower and is time-consuming and consequently very expensive. Referring to this balancing of a supercritical operating rotor supported in AMBs marks a specific challenge.

The aim of the research described in this paper is a partial automation of the balancing process. Manpower and time effort should be significantly decreased by the combination of the AMBs with active balancing devices (ABDs). Saturation of the AMBs must be avoided and the vibration level must be minimized to reach the supercritical operating speed.

Section II gives an overview of the AMB basics and explains the unbalance control facility. Afterwards a suitable ABD is presented in Section III, which will be combined with the AMBs. In Section IV the test rig is shown and described. The dynamic behavior of the rotor, presented in Section V, is essential for a safe supercritical operation and it is also the basis for possible balancing methods described in Section VI. The experimental results are given in Section VII followed by the conclusion in Section VIII.

II. AMBs and Unbalance Control

Active magnetic bearings have been deployed for years for the contactless suspension of rotating machine parts. Due to their operating principle - maintaining a hovering rotor by means of only magnetic forces - some basic advantages arise compared to other bearing technologies: No friction and thus no wear, no need for lubricants and lubricant systems, longer service intervals, no process contamination are only the most important benefits. Active magnetic bearings can be applied to rotors with very high rotation speeds and high power density. They can operate also under extreme environmental conditions such as high vacuum or high temperature.

A rotor with unbalance exerts unbalance forces on the machine housing. These forces cause vibrations and audible noise emissions. Due to unbalance the synchronous coil currents become big at high rotation speeds and amplifier saturation can occur. In the control of AMBs this problem is addressed by unbalance force rejection control (UFRC). UFRC aims at letting the rotor spin about its principal axis of inertia. Consequently no unbalance forces are transmitted to the housing and synchronous coil currents are eliminated completely. UFRC sometimes is called "unbalance compensation" or "autobalancing" whereas the last expression is rather misleading, since not the unbalance of the rotor is eliminated but its impact on other machine parts.

If a rotor has significant unbalance the displacement of the rotor (orbits) may become large once UFRC is activated. Of course the orbits must remain smaller than the catcher bearing air gap at any time. Therefore proper balancing of the rotor is most often inevitable despite UFRC. Balancing of rotors is usually done by adding or removing of small masses at particular locations. As already mentioned this is a rather time consuming and costly process. In Section III a device, which allows changing the unbalance state of a rotor under operating conditions, will be presented. Since the above mentioned UFRC estimates continuously the rotor unbalance, the combination of the

*This research is supported by the GROWTH Project MagFly (GRD1-2001-40191).

balancing device and the AMB yield an online closed-loop active balancing system. The estimated rotor unbalance can be used as command signal for the balancing device. The implementation of UFRC is discussed more in detail.

A survey of different UFRC structures is given in [1]. The compensation structure in [1] is based on the insertion of a so-called generalized notch filter into the control loop shown in Fig. 1. This dynamic system computes a sinusoidal, synchronous compensation signal, which is subtracted from the sensor signal. Amplitude and phase of this signal are continuously adapted such that the synchronous component is perfectly "filtered" from the sensor signal. Note that there is no notch filter put in the closed-loop, which may destroy closed-loop stability and thus must be taken into account in the design of the position controller. The synchronous compensation signal c in Fig. 1 is generated by the feedback block N_f. The input of N_f is the controller input e, which is the difference between the sensor signal y and c. Suppose that the signal y contains a sinusoidal component of frequency Ω. The input of N_f is multiplied by $\sin(\Omega t)$ and $\cos(\Omega t)$. Since the two operands have the same fundamental frequency, the frequency Ω of signal e is shifted to frequency zero[1]. The two signals are multiplied by the transformation matrix T. This matrix essentially determines closed-loop stability. When properly chosen stability is guaranteed. Since only the DC components are of interest the signals are then passed through integrators. The compensation signal c is the sum of the integrator states x_1 and x_2 multiplied by $\sin(\Omega t)$ and $\cos(\Omega t)$, which shifts the DC signals back to frequency Ω. The integrators actually act as controllers for the DC component of the transformed signals. Given the system is stable, the integrator inputs converge to zero. It is obvious that the integrator states represent the run out of the rotor due to unbalance. In this sense UFRC is an estimator of the rotor unbalance. The orbit radius is given by $r_u = 0.5 \cdot \sqrt{x_1^2 + x_2^2}$. A disadvantage of the presented

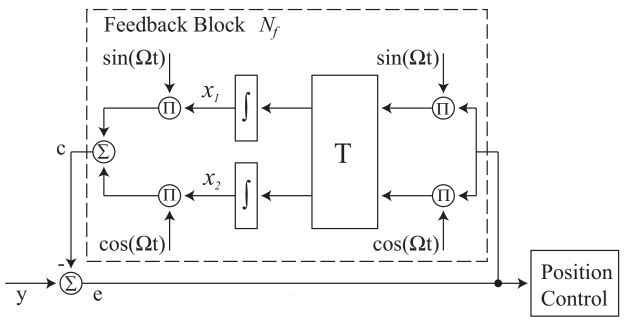

Fig. 1. UFRC Implementation: Feedback Structure N_f

URFC is the fact, that close to and at critical rotor speeds synchronous damping is needed and thus the URFC must be deactivated. Consequently also the estimation of rotor unbalance is disabled at these frequencies.

III. Active balancing devices

An extensive review of active balancing and vibration control of rotating machinery is given in [2]. Active magnetic bearings and active balancing devices are classified as facilities for active balancing. Here both tools are combined. For an on-line variation of a rotor's unbalance state a contactless operation of these tools is essential. The *Hofmann - EMB 7000 Ringbalancer* fulfills this main requirement. Fig. 2 gives an overview of the system.

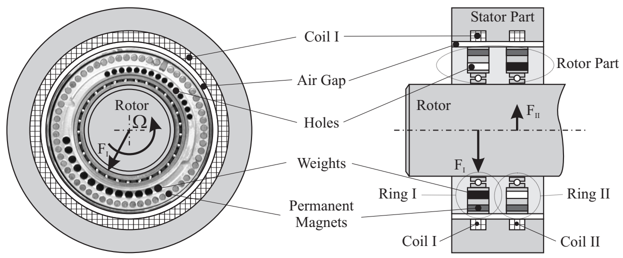

Fig. 2. Ringbalancer System

The shaft is equipped with two of these systems like shown in Fig. 6. One *Ringbalancer* system consists of a rotor part, which is mounted on the shaft and a stator part. In common applications they are arranged in a centric position with a constant air gap of $0.5\,\mathrm{mm}$. This ABD uses a mass redistribution system consisting of two rings I and II, which are suspended on thin-section bearings, each with a certain balancing mass m [3]. The basic mode of operation is shown in Fig. 3. The axial distance between the two rings is neglected thus it can be viewed as one balancing plane. The rings are held in place relative to the rotor by permanent magnets. The magnitude and position of the balancing mass in one plane is a result of the two rings' position so it can be changed by moving the two rings. The position of each ring is not free and continuously variable on the orbit. They are moved in steps of $6°$, which is done electromagnetically similar to a stepper drive within seconds. The stator part includes two coils to generate the magnetic flux, one for each ring. A maximum unbalance of $200\,\mathrm{gmm}$ can be generated by each *Ringbalancer*.

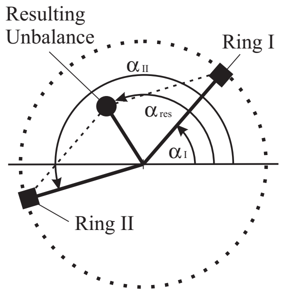

Fig. 3. *Mode of Operation*

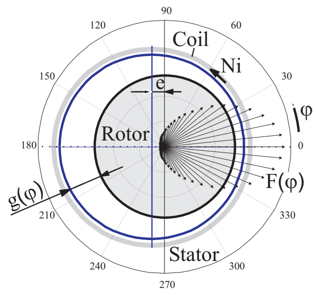

Fig. 4. *Eccentric Operation*

[1]The multiplication in time domain corresponds to a convolution in frequency domain. This fact may help to understand the statement.

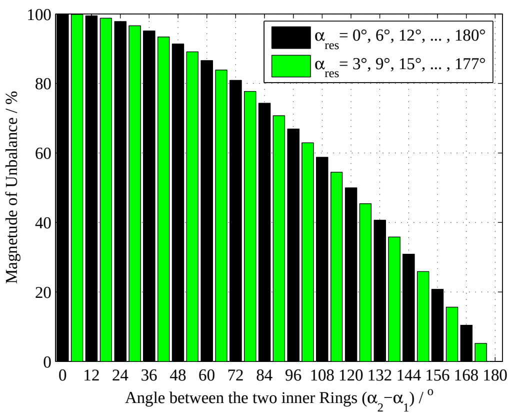

Fig. 5. Characteristic Diagram of the Actuator (100 % $\equiv$ 200 gmm)

For the operation at the test rig the *Ringbalancers* are modified. In contrast to their common application where the air gap is constant on the orbit, here it is a function of the position φ, which is a result of the shaft's motion described in Section II. An unwanted effect is the electromagnetic force $F(\varphi)$ illustrated in Fig. 4, which excites the shaft during operation of the *Ringbalancer*. The force is inversely proportional to the square of the air gap $g(\varphi)$ and so a function of φ. Furthermore the air gap has to be extended to $1.5\ \mathrm{mm}$ to avoid rubbing between rotor and stator parts. A proper operation of the *Ringbalancer* system under mentioned conditions had been attested in [3].

The characteristic diagram of the actuator is given in Fig. 5. It shows the magnitudes of unbalances that can be generated at the angular positions α_{res}. The grid of the positions of the unbalance is equidistant unlike the grid of the magnitude. The smallest unbalance, that can be generated by the actuator, is already more than 5.2 % of the total unbalance of $200\ \mathrm{gmm}$. Near the actuator capacity the steps of change decrease to 0.14 %.

IV. Test rig

Fig. 6 and Fig. 7 show the test rig that was constructed to investigate *Magnetic Bearings in Aero Engines* and is part of the EU-project *MagFly*. The experimental rig consists of a low pressure shaft of a helicopter engine radially supported by AMBs. Fig. 6 illustrates the shaft in detail. The hollow shaft has a diameter of $25\ \mathrm{mm}$ and a wall thickness of $3.5\ \mathrm{mm}$ and includes two turbine stages with removed blades. With a length of $1050\ \mathrm{mm}$, the

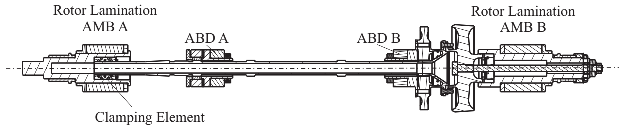

Fig. 6. Section of the Shaft

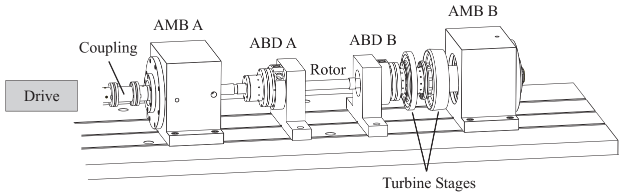

Fig. 7. Test Rig

overall weight is approximately $23\ \mathrm{kg}$. The outer regions of the shaft had been redesigned for carrying the rotor laminations, which are part of the AMBs. Two ABDs are mounted on the shaft, one in the compressor and one in the turbine region. Using these, it is possible to balance the shaft. The rotor parts of the ABDs must be assembled to the rotor along the axial direction because they are radially indivisible ring elements. Hence it is necessary to split the shaft in two parts to allow the assembly of the system. By using a clamping sleeve it is possible to connect and disconnect the two shaft parts in the region of the lamination of AMB A as shown in Fig. 6.

The shaft is fixed to a high speed drive with a torsionally stiff shaft coupling. The coupling compensates for possible angular and radial misalignment between the drive's shaft and the test section of the helicopter engine. It decouples the shaft in axial and radial directions, and disturbances from the drive do not affect the AMB-rotor system. The high speed drive consists of an induction motor controlled by a frequency converter and permits speeds up to $500\ \mathrm{Hz}$, which is in the supercritical speed range of the system. Containments are placed over all sensitive regions of the rig.

V. Rotordynamics

In focus now is the dynamic behavior of the shaft, which is the central element in the rig. Linear system behavior is assumed, thus it can be described completely by its natural frequencies, mode shapes and modal damping. For complex shaft designs these characteristic parameters can be calculated by the use of the finite element method. In case of actively levitated rotors excitations by the AMBs can occur, which have an effect on modes above the rotary speed Ω [4]. Due to this the shaft's dynamic behavior is analyzed up to $1000\ \mathrm{Hz}$, which is roughly four times the maximum rotating speed Ω. The results of this calculation are shown in Fig. 8. For the calculations the radial bearing stiffness and the radial stiffness of the coupling at the connection to the drive are neglected. Hence a free-free condition of the rotor is assumed, what is close to the real condition of AMB supported rotors. The mass of the coupling is implemented in the finite element model, which is fitted via modal analysis measurements. The mode shapes illustrate the high dynamic flexibility of the shaft in the center area. For a stable and robust operation collocation is desired. This means that the sensor location

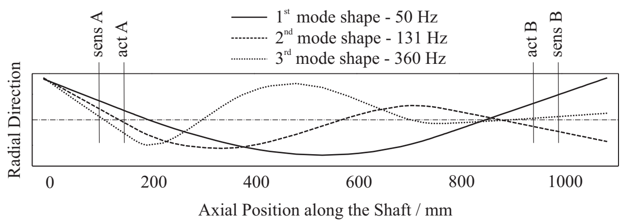

Fig. 8. Natural Frequencies and Mode Shapes of the Shaft

is the same as the actuator position. In real applications this is not given because of the axial extension of the magnetic bearing. At bearing A the mode shapes at ω_2 and ω_3 have nodes between the sensor and the actuator plane. Hence, a phase lag of $180°$ exists and the control loop becomes unstable if this fact is not regarded during the design of the control loop. The situation in bearing B is uncritical, because there a quasi-collocation exists.

One reason for these investigations is to avoid excitations of the shaft by the AMBs. Nevertheless the main excitation in the field of rotating machinery is the unbalance of the shaft. Characteristic for this excitation is that its frequency corresponds to the rotary speed Ω. This particularly relates to shafts in conventional bearings but also AMB supported shafts. Consequently the reduction of excitations caused by unbalance is desired. Therefore the knowledge of the shaft's dynamic behavior is more or less indispensable depending on the balancing method, which will be described in Section VI. It is essential to know the critical speeds, which must be passed through to reach the operating speed Ω. In these frequency ranges a good balancing state of the rotor yields to a maximum benefit concerning the reduction of unbalance-induced vibration. Fig. 9 shows a campbell diagram of the system for shaft speeds between 0 Hz and 500 Hz. The significant gyroscopic effect of the

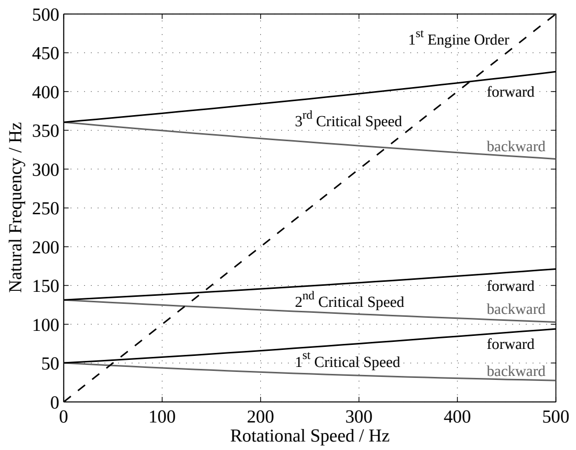

Fig. 9. Campbell Diagram of the Rotor

shaft yields forward and backward critical speeds, which are above and below their associated zero-running-speed natural frequencies [5]. In the case of unbalance only the forward critical speeds are excited. The rotor moves around an orbit with a static deformation. This is exceedingly dangerous because there is no effect of internal rotor damping. Other excitations, e.g. resulting of AMBs, can have a significant effect in the backward critical speeds. Unlike the unbalance-induced excitation here also high order harmonics excite the structure.

VI. Balancing of flexible rotors

For balancing of flexible rotors two different methods are known. The modal balancing method is based on the knowledge of the rotor's natural frequencies and mode shapes. Each mode is balanced at the corresponding natural frequency ω_i with a set of masses specifically selected so as not to disturb previously balanced lower modes [2]. Balancing of a mode with this method has an effect on the system over the entire speed range. Additional balancing steps at speeds, which are not close to a resonance do not have a significant effect.

Another experimental balancing method is called the influence coefficient method. It bases only on a linear system behavior and by contrast to the modal balancing method, knowledge of the rotor's modal nature is not necessary in detail. There are no restrictions for choosing balancing speeds but the effect of the method is limited to the frequency, at which the balancing is done. Again it makes sense to balance the rotor at frequencies close to its flexible modes because this way the highest effect can be achieved. However further balancing steps at uncritical speeds e.g. at the operating speed are possible and effective. For a safe run up through the critical speeds, a minimum of three balancing steps is advised: One at each critical speed and one at the operating speed. The basis of the influence coefficient method is explained by

$$\underline{\boldsymbol{w}}^{MP} = \underline{\boldsymbol{A}}\underline{\boldsymbol{U}}^{N} \tag{1}$$

with the unbalances $\underline{\boldsymbol{U}}^{N}$ in the planes N and the resulting displacements $\underline{\boldsymbol{w}}^{MP}$ in the measurement points MP [6]. The number of measurement points is

$$MP = SP \cdot MS \tag{2}$$

with the available number of sensor planes SP and the measurement speeds MS. The elements of matrix $\underline{\boldsymbol{A}}$ are the influence coefficients

$$\underline{\alpha}_{ik} = \frac{\underline{w}_{ik} - \underline{w}^{0}}{\underline{U}_{k}} \qquad i,k = 1,2,...,N \tag{3}$$

where $\underline{w}_{ik}$ are the displacements at measurement points i due to an unbalance $\underline{U}_k$ at plane k. $\underline{w}^0$ are the displacements at the measurement points i of the initial rotor state without any test unbalance. With the knowledge of matrix $\underline{\boldsymbol{A}}$, the requirement det $\underline{\boldsymbol{A}} \neq 0$ and the displacements $\underline{\boldsymbol{w}}^{MP}$ at all measurements points MP the wanted set of unbalances is

$$\underline{\boldsymbol{U}}^N = \underline{\boldsymbol{A}}^{-1}\underline{\boldsymbol{w}}^{MP}. \tag{4}$$

If $-\underline{\boldsymbol{U}}^N$ is applied to the rotor, the displacements in the sensor planes SP at the measurement speeds MS will be zero. To reach this, the matrix $\underline{\boldsymbol{A}}$ must be identified. It can be seen as a set of transfer functions referring to unbalances and their effects in the sensor planes. A total of $N+1$ measurements is necessary to identify all $MP \cdot N$ elements of matrix $\underline{\boldsymbol{A}}$ by observance of N planes. Therefore it is necessary to add test weights at the balancing planes - hence the rotor must be stopped $N+1$ times. Fig. 10 illustrates the procedure using constant correction masses. To minimize the displacements in the two sensor planes at two critical speeds $\Omega_{1,2}$ four balancing planes are needed. The number of necessary balancing planes increases with the critical speeds, which must be passed. For the case Ω_2 cannot be reached without a pre-balancing at Ω_1 the procedure must be accomplished stepwise.

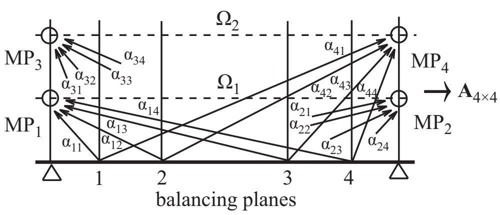

Fig. 10. Identification of Influence Coefficients - Common Procedure

By using the *Ringbalancer* systems these stops during the run-up of the shaft speed are not longer necessary. All test unbalances can be generated by the ABDs during operation. Furthermore, Fig. 11 shows that two balancing planes equipped with two ABDs are sufficient for passing several critical speeds, assuming the *Ringbalancers* can provide sufficient unbalance. With a decreasing number of balancing planes also the number of influence coefficients decreases what minimizes the measurement effort. The balancing procedure must be applied in steps because two ABDs are able to balance the rotor at one critical speed for two sensor planes. If this critical speed has been passed, the same ABDs can be used for balancing at the following speed. All identified balancing sets must be saved and rearranged before passing the critical speeds during further operation of the rotor.

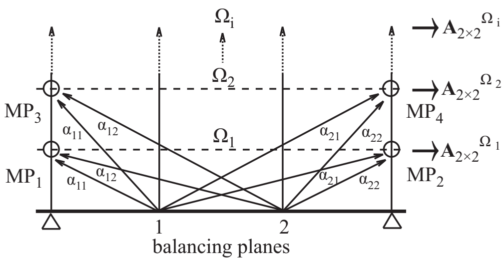

Fig. 11. Identification of Influence Coefficients - Using ABDs

VII. Experimental results

In this Section test setups are explained and the test results will be presented. Subsection VII-A describes active balancing using the information of displacements from the URFC described in Section II. In Subsection VII-B this information is taken from the original sensor signals. In both cases run-up tests from 0 Hz to 170 Hz will be taken to evaluate the operation of the system under varying speed conditions.

A. Balancing using the UFRC

Before the run-up test, the matrix $\underline{\boldsymbol{A}}$ must be identified. Therefore the URFC is activated. The measurements are carried out at 10 speeds in the range from standstill up to 170 Hz. Each of these measurements takes approximately 60 sec. After the full identification of matrix $\underline{\boldsymbol{A}}$, a number of 10 balancing sets are calculated. An exception here is balancing set No. 8. In the interval between 117 Hz and 157 Hz the *Ringbalancers* are adjusted to a neutral position. That is necessary because the rotor is mechanically pre-balanced at a speed of 135 Hz. Arrows at the bottom of the run-up diagrams indicate the speed intervals and the matching balancing sets $(S1^*, S2^*, ...)$. All this information is saved and can be permanently recalled by the balancing system. Fig. 12 shows the radial displacements in bearing A with and without active balancing during a run-up. Below the 1^{st} critical speed the effect of active balancing is low. The reason for this is the limitation of the *Ringbalancers*: The unbalance, which was calculated here can not be generated. In the range between 69 Hz

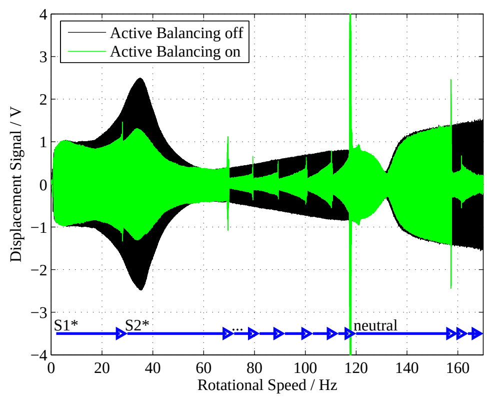

Fig. 12. Displacements in Bearing A - Run-up from 0 to 170 Hz

and 117 Hz and above 157 Hz a significant reduction of the displacements about 70 % can be detected. In the ranges of the critical speeds the URFC must be deactivated like mentioned in Section II. The consequence is that in these ranges no influence coefficients can be acquired and hence no balancing sets can be calculated. This is the main disadvantage because especially near the critical speeds a reduction of unbalance induced excitation is necessary. The main advantages using URFC is the accuracy and the fast availability of the unbalance information.

At the switching speeds, marked with the arrows, the eccentric operation of the ABDs described in Section III causes undesirable excitations, however they do not cause a system failure. It is important, especially close to the critical speeds, how the ABDs generate the necessary balancing set. If a bad ring position must be passed during the *Ringbalancers*' operation, the system fails and the rotor crashes.

B. Balancing using the original Sensor Signals

The necessity to balance the rotor near the critical speeds leads to the idea to use the original displacement signals from the AMBs. The speed synchronous excitations are dominant in the sensor signals, hence the effort for signal processing is low. The signals fluctuate slightly in contrast to the very stable information sensed by URFC. To increase the signal quality some averages are necessary. Consequently the time effort increases. The basic procedure to generate the matrix $\underline{\boldsymbol{A}}$ and to calculate suitable balancing sets is the same like in Subsection VII-A.

For the following tests, the rotor is not mechanically pre-balanced at 135 Hz. Fig. 13 illustrates the radial displacements of bearing A during a run-up test. The displacements without active balancing rises significantly near the 2^{nd} critical speed. It is not possible to pass this speed, because the rotor touches the emergency bearings. The use of active balancing allows to pass the 2^{nd} critical speed. Here a reduction of displacements of approximately 90 % is achieved. In the ranges of the critical speeds

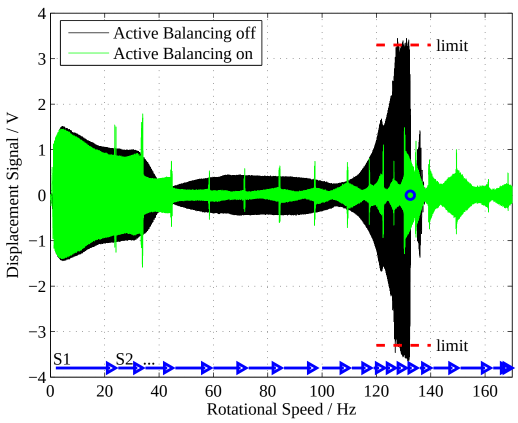

Fig. 13. Displacements in Bearing A - Run-up from 0 to 170 Hz

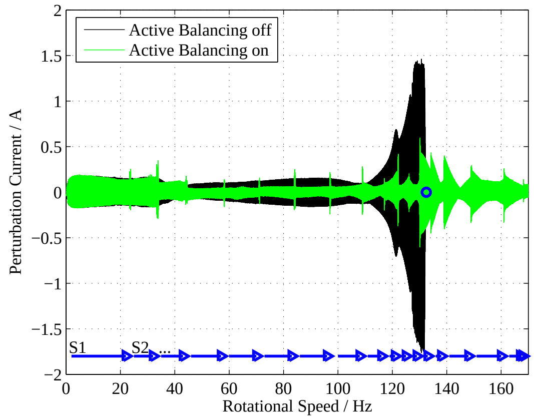

Fig. 14. Perturbation Current in Bearing A - Run-up from 0 to 170 Hz

the balancing sets must be adjusted very fast because of the fast increasing displacements. Active balancing now is possible at each speed with at least the effect as was reached in Subsection VII-A. Again the low effect below the 1^{nd} critical speed is because of the actuator limitation. Fig. 14 verifies the proper operation of active balancing on the basis of the perturbation current in the coils of bearing A. Also in the current signal the effect of active balancing is significant.

VIII. Conclusion

This paper presents an on-line closed-loop active balancing facility for a supercritical rotor on AMBs. The combination of AMBs and ABDs allows to pass critical rotor speeds. The displacements and the AMB perturbation currents decrease significantly. Furthermore a partial automation of the balancing process is reached and hence a reduction of manpower and time effort.

References

[1] R. Herzog, P. Bühler, C. Gähler and R. Larsonneur, "Unbalance compensation unsing generalized notch filters in the multivariable feedback of magnetic bearings," IEEE Transactions on Control Systems Technology, vol. 4, no. 5, pp. 580-586, September 1996.

[2] S.Zhou and J. Shi, "Active balancing and vibration control of rotating machinery: A survey," The Shock and Vibration Digest, vol. 33, no. 4, pp. 361-371, July 2001.

[3] K. Adler, D. Neumeuer and R. Nordmann, "Active unbalance generation for failure simulation in turbo engines," ACTIVE04 - The 2004 International Symposium on Active Control of Sound and Vibration, September 2004.

[4] T. Krüger, M. Aenis, D. Neumeuer, U. Schönhoff and R. Nordmann, "Modellbildung und Reglerentwurf zu aktiven Magnetlagersystemen für elastische Rotoren," Schwingungen in rotierenden Maschinen V, February 2001.

[5] D. Childs, "Turbomachinery rotordynamics," Wiley-Interscience, New York · Chichester · Brisbane · Toronto · Singapore, 1993.

[6] A. Lingener, "Auswuchten - Theorie und Praxis," Verlag Technik, Berlin · München, 1992.